

A relativistic model of the topological acceleration effect

Jan J. Ostrowski, Boudewijn F. Roukema and Zbigniew P. Buliński

Toruń Centre for Astronomy, Nicolaus Copernicus University,
ul. Gagarina 11, 87-100 Toruń, Poland

Abstract. It has previously been shown heuristically that the topology of the Universe affects gravity, in the sense that a test particle near a massive object in a multiply connected universe is subject to a topologically induced acceleration that opposes the local attraction to the massive object. This effect distinguishes different comoving 3-manifolds, potentially providing a theoretical justification for the Poincaré dodecahedral space observational hypothesis and a dynamical test for cosmic topology. It is necessary to check if this effect occurs in a fully relativistic solution of the Einstein equations that has a multiply connected spatial section. A Schwarzschild-like exact solution that is multiply connected in one spatial direction is checked for analytical and numerical consistency with the heuristic result. The T^1 (slab space) heuristic result is found to be relativistically correct. For a fundamental domain size of L , a slow-moving, negligible-mass test particle lying at distance x along the axis from the object of mass M to its nearest multiple image, where $GM/c^2 \ll x \ll L/2$, has a residual acceleration away from the massive object of $4\zeta(3)G(M/L^3)x$, where $\zeta(3)$ is Apéry's constant. For $M \sim 10^{14}M_\odot$ and $L \sim 10$ to $20h^{-1}$ Gpc, this linear expression is accurate to $\pm 10\%$ over $3h^{-1}$ Mpc $\lesssim x \lesssim 2h^{-1}$ Gpc. Thus, at least in a simple example of a multiply connected universe, the topological acceleration effect is not an artefact of Newtonian-like reasoning, and its linear derivation is accurate over about three orders of magnitude in x .

PACS numbers: 98.80.Jk, 98.80.Es, 04.20.Gz, 02.40.-k

1. Introduction

The topology of spatial sections of the Universe has been of interest since the foundations of relativistic cosmology (e.g., de Sitter, 1917; Friedmann, 1923, 1924; Lemaître, 1927; Robertson, 1935)[‡]. However, astronomical measurements aimed at determining spatial topology have long suffered a theoretical disadvantage compared to curvature measurements. The latter are tightly related to another type of astronomical measurement (matter-energy density) via a well-established physical theory: general relativity. Some elementary work that might lead to a physical theory of cosmic topology has been carried out, by comparing certain characteristics of different manifolds (Seriu, 1996; Anderson et al., 2004) and by explorations of some elements of topology change in quantum gravity (e.g., Dowker and Surya, 1998), but these remain very distant from astronomical observations. Thus, most of the empirical work of the past few decades has been carried out with no theoretical constraints, apart from assuming Friedmann-Lemaître-Robertson-Walker (FLRW) cosmological models. For recent empirical analyses of the case for and against a multiply connected positively curved spatial section, in particular the Poincaré dodecahedral space S^3/I^* , see Roukema and Kazimierczak (2011) and references therein. Theoretical developments could offer the possibility of new astronomical tests for cosmic topology.

For perfectly homogeneous solutions of the Einstein equations, i.e. FLRW models, if the sign of the curvature is determined empirically, only the covering space H^3 , \mathbb{R}^3 , or S^3 , i.e. an apparent space containing many copies of the fundamental domain, can be inferred. The 3-manifold of comoving space itself, i.e. H^3/Γ , \mathbb{R}^3/Γ , or S^3/Γ , respectively, for a fundamental group (holonomy group) Γ , is not implied by the curvature. However, heuristic, Newtonian-like calculations have recently shown that the presence of a single inhomogeneity is enough to, in principle, distinguish different possible spaces of the same fixed curvature (Roukema et al., 2007; Roukema and Rózański, 2009). The effect is a long-distance, globally induced acceleration term that opposes the local attraction to a massive object. Curiously, the effect, (hereafter, “topological acceleration”[§]) is much weaker in the Poincaré dodecahedral space than in other spaces, hinting at a theoretical reason for selecting this space independent of the observational reasons published six years earlier.

Astronomical tests for cosmic topology are almost always based on the fact that photons from a point in comoving space can arrive at the observer by multiple paths (e.g. Roukema, 2002). In contrast, topological acceleration has the potential to provide tests of galaxy kinematics that could provide experimental constraints on cosmic topology independent of tests based on multiple imaging (of extragalactic objects or of cosmic microwave background temperature fluctuations). However, the calculations of the effect (Roukema et al., 2007; Roukema and Rózański, 2009) did not use full solutions

[‡] See Lemaître (1931) for an incomplete translation of Lemaître (1927).

[§] The implied meaning is “acceleration induced globally by cosmic topology”; a term used in earlier work is “residual gravity”.

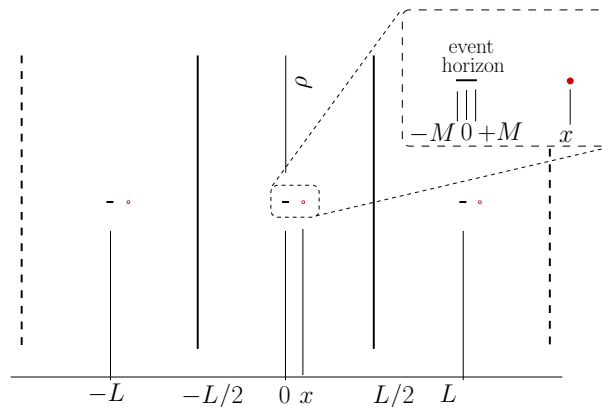


Figure 1. Event horizon of massive object of mass M (dark line segment) and test particle (dot) in slab space T^1 of fundamental domain length L . In a 3-section of constant coordinate time t , the event horizon of the massive object is spherically symmetric in terms of the metric, but in the Weyl coordinates used here, it is a line segment extending from $-M$ to $+M$ in the x direction, where $G = c = 1$, and is of zero size in the radial coordinate ρ . The test particle is displaced a small distance from the massive object, i.e. $x \ll L/2$, but well outside the event horizon, i.e. $0 < M \ll x$ (zoom) [Eq.(2)].

of the Einstein equations. The FLRW metric is an exact solution of the Einstein equations, but it can only be applied to the real Universe as a heuristic guide, since galaxies (inhomogeneities) exist. When this heuristic guide is used to interpret recent observational constraints, an accelerating scale factor and dark energy are inferred. That is, the latter appear to be artefacts of a heuristic approach (e.g. C el erier et al., 2010; Buchert and Carfora, 2003; Wiegand and Buchert, 2010). Similarly, since a heuristic, Newtonian-like approach was used to calculate the topological acceleration effect, the latter could, in principle, also be an artefact. Thus, it is important to check whether the effect really exists in the relativistic case of a $(3 + 1)$ -dimensional spacetime with multiply connected spatial sections.

Here, we compare the heuristic calculation of Roukema et al. (2007) for T^1 (slab space, i.e. $S^1 \times \mathbb{R}^2$) to a limiting case of an exact, Schwarzschild-like solution which has a T^1 spatial section outside of the event horizon. In Sect. 2.1 we list the simplifying assumptions for considering a test particle distant from the event horizon but much closer to the “first” copy of a massive object than to an “adjacent” copy. The metric in Weyl coordinates and related functions (Korotkin and Nicolai, 1994) are given in Sect. 2.2 for an analytical derivation and the numerical method is stated in Sect. 3.2. The analytical and numerical calculations are presented in Sect. 3.1 and Sect. 3.2, respectively, and a conclusion is given in Sect. 5.

2. Method

For the Newtonian-like calculation, Fig. 3 of Roukema et al. (2007) illustrates the situation of a test particle at distance x from a point object of mass M in T^1 , lying along

the spatial geodesic of length L from the massive object to itself. Defining $\epsilon := x/L$ gives the topologically induced acceleration (Eq. (7), Roukema et al., 2007)

$$\ddot{x} = M \sum_{j=1}^{\infty} \left[\frac{1}{(jL-x)^2} - \frac{1}{(jL+x)^2} \right] \approx 4.8 \frac{M\epsilon}{L^2} \quad (1)$$

when $\epsilon \ll 1$, adopting $G = 1$.

2.1. Assumptions

A Schwarzschild-like solution of the Einstein equations has an event horizon, but behaviour close to the event horizon (or inside it) is not of interest here. Also, if the topological acceleration effect were to be analysed for its effects on galaxy dynamics, peculiar velocities would typically be of the order of $10^{-3}c$ and very rarely exceed $10^{-2}c$. As in the earlier derivation of Eq. (1), we consider a test particle lying along the closed spatial geodesic joining the massive object to itself, i.e. having Weyl radial coordinate $\rho = 0$.

Thus, in addition to adopting the conventions $G = c = 1$, a $(-, +, +, +)$ metric, Greek spacetime indices $0, 1, 2, 3$ and Roman space indices $1, 2, 3$, our assumptions become:

$$0 < M \ll x \ll L/2, \quad (2)$$

$$\frac{dx^i}{dt} \ll 1 \Rightarrow \frac{dx^i}{d\tau} \ll 1 \lesssim \frac{dt}{d\tau}, \quad (3)$$

$$\rho = 0, \quad (4)$$

where τ is the proper time along the test particle's world line $x^\alpha(\tau)$, and $t \equiv x^0$. The assumption of a low coordinate velocity implies a low 4-velocity spatial component [Eq. (3)].

2.2. Analytical approach

Korotkin and Nicolai (1994) presented a family of multiply connected exact solutions of the Einstein equations that includes a Schwarzschild-like solution with T^1 spatial sections outside of the event horizon. Figure 1 shows this solution in Weyl coordinates x and ρ . Using Weyl coordinates and the Ernst potential, the metric is

$$ds^2 = -e^\omega dt^2 + e^{-\omega} [e^{2k}(dx^2 + d\rho^2) + \rho^2 d\phi^2] \quad (5)$$

from Eq. (9) of Korotkin and Nicolai (1994),^{||} where k and ω relate to an Ernst potential ϵ defined on $\xi := x + i\rho$, with

$$\epsilon_0(x, \rho) := \frac{\sqrt{(x-M)^2 + \rho^2} + \sqrt{(x+M)^2 + \rho^2} - 2M}{\sqrt{(x-M)^2 + \rho^2} + \sqrt{(x+M)^2 + \rho^2} + 2M} \quad (6)$$

^{||} In the online version 1 of arXiv:gr-qc/9403029, the time component has an obvious typological error in the sign.

$$\omega_0 := \ln \varepsilon_0, \quad a_0 := 0, \quad a_{j \neq 0} := \frac{2M}{L|j|} \quad (7)$$

$$\omega(x, \rho) := \sum_{j=-\infty}^{\infty} [\omega_0(x + jL, \rho) + a_j], \quad \varepsilon := e^\omega \quad (8)$$

$$\partial_\xi k = 2i\rho \frac{\partial_\xi \varepsilon \partial_\xi \bar{\varepsilon}}{(\varepsilon + \bar{\varepsilon})^2}, \quad (9)$$

from Eqs (13), (12), (5) and (7) of Korotkin and Nicolai (1994).[¶] The Ernst potential is real for this solution, so Eq. (9) gives

$$\partial_\xi k = \frac{1}{2}i\rho \frac{(\partial_\xi \varepsilon)^2}{\varepsilon^2} = \frac{1}{2}i\rho [\partial_\xi (\ln \varepsilon)]^2 = \frac{1}{2}i\rho (\partial_\xi \omega)^2. \quad (10)$$

Thus, at $\rho = 0$, we have $\partial_\xi k = 0$, i.e. k is a constant along $\rho = 0$. We choose $k(\rho = 0) = 0$, since any other value just implies a rescaling of units. Thus, the metric on $\rho = 0$ is

$$ds^2 = -e^\omega dt^2 + e^{-\omega} (dx^2 + d\rho^2 + \rho^2 d\phi^2). \quad (11)$$

Defining the tangent vector \vec{V} by components $V^\alpha := dx^\alpha/d\tau$, the geodesic equation for the test particle is $\nabla_V \vec{V} = \vec{0}$, i.e.

$$\frac{d^2 x^\alpha}{d\tau^2} + \Gamma^\alpha_{\beta\gamma} \frac{dx^\beta}{d\tau} \frac{dx^\gamma}{d\tau} = 0, \quad (12)$$

where $\Gamma^\alpha_{\beta\gamma}$ are the Christoffel symbols of the second kind.⁺ Since a $(-, +, +, +)$ convention is used and low velocities are assumed [Eq. (3)], coordinate and proper time are related by

$$d\tau^2 = |g_{00}| (dx^0)^2 = e^\omega dt^2, \quad (13)$$

giving the x^1 coordinate acceleration

$$\frac{d^2 x^1}{dt^2} = \frac{d^2 x}{dt^2} = e^{-\omega} \frac{d^2 x}{d\tau^2}. \quad (14)$$

Given the conditions in Eqs. (2), (3), and (4) and the Ernst potential expressions in Eqs. (11), (6), (7), and (8), conversion to metric units of x and t would only modify this to second order. In Sect. 3.1, $d^2 x/dt^2$ is evaluated.

2.3. Numerical approach

The Ernst potential expressions [Eqs (6), (7), and (8)] are used for numerical evaluation of Eq. (20) (below) by finite differencing over small intervals. A typical cluster of galaxies has a mass of $\sim 10^{14} M_\odot$, i.e. $M = 4.78$ pc in length units, and the most massive clusters have masses up to about $10^{15} M_\odot$.^{*} Observational estimates of L are

[¶] Positive square roots are implied in Eq. (6).

⁺ Symmetric definition.

^{*} In the Weyl coordinate x , the event horizon occurs along $|x| \leq M$, $\rho = 0$ (Fig. 1, which may seem surprising given that the event horizon in Schwarzschild coordinates occurs at $r = 2M$. See Frolov and Frolov (e.g., 2003, Sect. II.B. and references therein) for the relation between Weyl and Schwarzschild coordinates.

in the range 10 to $20h^{-1}$ Gpc (e.g. Roukema and Kazimierczak, 2011, and references therein). Thus, typical scales of M/L of interest should be $M/L \sim 10^{-10}$ to 10^{-8} . Since M/x , M/L , and x/L are small, the use of 53-bit-significant double-precision floating-point numbers is replaced by arbitrary precision arithmetic, for $10^{-10} < M/L < 10^{-8}$. These calculations are presented in Sect. 3.2.

3. Results

3.1. Coordinate acceleration

Given that the test particle is far from the “close” copy of the event horizon and from “distant” copies [Eq. (2)], we have $|\Gamma^\alpha_{\beta\gamma}| \ll 1$. Together with Eq. (3), this implies that most of the terms in the sum in Eq. (12) are small terms of second order or higher, leaving

$$\frac{d^2x^\alpha}{d\tau^2} + \Gamma^\alpha_{00} \left(\frac{dx^0}{d\tau} \right)^2 \approx 0. \quad (15)$$

Since the metric is static (and diagonal), we have

$$\Gamma^\alpha_{00} = \frac{1}{2} g^{\alpha\lambda} (\partial_0 g_{\lambda 0} + \partial_0 g_{0\lambda} - \partial_\lambda g_{00}) = -\frac{1}{2} g^{\alpha\lambda} \partial_\lambda g_{00}. \quad (16)$$

Using Eq. (13), Eq. (15) becomes

$$\frac{d^2x^\alpha}{d\tau^2} = \frac{1}{2} \frac{g^{\alpha\lambda}}{|g_{00}|} \partial_\lambda g_{00}. \quad (17)$$

Since the metric is diagonal, we have $g^{xx} = (g_{xx})^{-1} = e^{+\omega}$ and

$$\frac{d^2x^1}{d\tau^2} = \frac{1}{2} \frac{g^{11}}{|g_{00}|} \partial_1 g_{00}, \quad (18)$$

i.e.,

$$\frac{d^2x}{d\tau^2} = \frac{1}{2} \frac{g^{xx}}{|g_{tt}|} \partial_x g_{tt} = \frac{1}{2} \frac{e^\omega}{e^\omega} (-\partial_x e^\omega) = -\frac{1}{2} e^\omega \partial_x \omega. \quad (19)$$

Thus, from Eq. (14),

$$\frac{d^2x}{dt^2} = -\frac{1}{2} \partial_x \omega. \quad (20)$$

Substituting Eqs (7) and (6) in Eq. (8a) and using Eq. (2),

$$\begin{aligned} \omega(x, \rho) &= w_0(x, \rho) + \sum_{j=-\infty, j \neq 0}^{\infty} \left[\omega_0(x + jL, \rho) + \frac{2M}{L|j|} \right] \\ &\approx w_0(x, \rho) + \sum_{j=-\infty, j \neq 0}^{\infty} \omega_0(x + jL, \rho) \end{aligned} \quad (21)$$

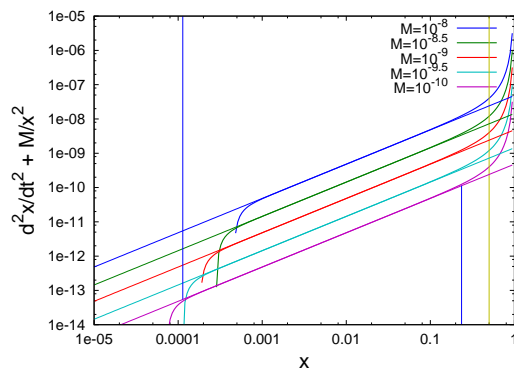


Figure 2. Topological acceleration $d^2x/dt^2 + M/x^2$ as a function of coordinate distance x from the “first” copy of the massive object of mass M , along the spatial geodesic joining the massive object to itself, using Eqs (6), (7), and (8) in Eq. (20), for $L = 1$. The curves show masses from $M = 10^{-10}$ to 10^{-8} , from bottom to top, respectively, as labelled. The sloping lines show $4\zeta(3)(M/L^3)x$. The vertical line at $x = 0.5$ shows the halfway point to the “next” copy of the massive object. The vertical lines down to and up to the $M = 10^{-10}$ curve show the range over which the linear approximation is valid to within $\pm 10\%$.

Dropping the ρ dependence since we are interested in the $\rho = 0$ axis, the derivative can be written using Eq. (7)

$$\begin{aligned}
 \partial_x \omega(x) &= \partial_x \left[\ln \varepsilon_0(x) + \sum_{j=-\infty, j \neq 0}^{\infty} \ln \varepsilon_0(x + jL) \right] \\
 &= \frac{\partial_x \varepsilon_0(x)}{\varepsilon_0(x)} + \sum_{j=1}^{\infty} \frac{\partial_x \varepsilon_0(x + jL)}{\varepsilon_0(x + jL)} + \sum_{j=1}^{\infty} \frac{\partial_x \varepsilon_0(x - jL)}{\varepsilon_0(x - jL)} \\
 &= \frac{\partial_x \varepsilon_0(x)}{\varepsilon_0(x)} + \sum_{j=1}^{\infty} \frac{\partial_x \varepsilon_0(x + jL)}{\varepsilon_0(x + jL)} - \sum_{j=1}^{\infty} \frac{\partial_x \varepsilon_0(jL - x)}{\varepsilon_0(jL - x)} \\
 &\approx \partial_x \varepsilon_0(x) + \sum_{j=1}^{\infty} \partial_x \varepsilon_0(jL + x) - \sum_{j=1}^{\infty} \partial_x \varepsilon_0(jL - x),
 \end{aligned} \tag{22}$$

where the third equality follows from using $\partial_{x'} \varepsilon_0(-x') = -\partial_{x'} \varepsilon_0(x')$ [cf. Eq. (6)], and the approximation follows from using Eqs (2), (4), and $j \geq 1$ in Eq. (6).

For $0 < M < x'$, Eq. (6) simplifies to

$$\varepsilon_0(x', 0) = \frac{x' - M}{x' + M}. \tag{23}$$

Again defining $\epsilon := x/L$, we then have

$$\begin{aligned}
 \partial_x \omega(x) &\approx \frac{2M}{(x + M)^2} + \sum_{j=1}^{\infty} \frac{2M}{(jL + x + M)^2} - \sum_{j=1}^{\infty} \frac{2M}{(jL - x + M)^2}
 \end{aligned}$$

Table 1. Minimum and maximum distance x for which the $4\zeta(3)(M/L^3)x$ approximation is accurate to within 10% (cf. Fig. 2).^a

M	10^{-10}	3×10^{-10}	10^{-9}	3×10^{-9}	10^{-8}
$\log_{10} x_{\min}$	-3.94	-3.77	-3.54	-3.37	-3.14
$\log_{10} x_{\max}$	-0.63	-0.63	-0.63	-0.63	-0.63
$\Delta \log_{10} x^b$	3.32	3.14	2.91	2.74	2.51

^aFor convenience, $L = 1$.

^bRange in $\log_{10} x$.

$$\begin{aligned}
 &\approx \frac{2M}{x^2} + \frac{2M}{L^2} \left(\sum_{j=1}^{\infty} \frac{1}{(j+\epsilon)^2} - \sum_{j=1}^{\infty} \frac{1}{(j-\epsilon)^2} \right) \\
 &\approx \frac{2M}{x^2} + \frac{2M}{L^2} \left[\sum_{j=1}^{\infty} \frac{1}{j^2} \left(1 - \frac{2\epsilon}{j} \right) - \sum_{j=1}^{\infty} \frac{1}{j^2} \left(1 + \frac{2\epsilon}{j} \right) \right] \\
 &= \frac{2M}{x^2} - \frac{8M}{L^2} \epsilon \sum_{j=1}^{\infty} \frac{1}{j^3} \\
 &= \frac{2M}{x^2} - \frac{8\zeta(3)M}{L^2} \epsilon
 \end{aligned} \tag{24}$$

where Eq. (2) is applied in the second and third lines, and $\zeta(3)$ is the Riemann zeta function evaluated at $\zeta = 3$, i.e. Apéry’s constant.

Hence, using Eq. (20),

$$\frac{d^2x}{dt^2} \approx -\frac{M}{x^2} + \frac{4\zeta(3)M}{L^2} \frac{x}{L} \approx -\frac{M}{x^2} + \frac{4.8M}{L^2} \frac{x}{L} \tag{25}$$

i.e. the coordinate acceleration is the Newtonian acceleration towards the local copy of the massive object plus an opposing topological acceleration term matching Eq. (1), i.e. the expression derived earlier in Roukema et al. (2007).

3.2. Numerical check

For $10^{-10} < M < 10^{-8}$, $L = 1$, $|j| \leq 14$, and linear offsets of $\delta x = \pm 10^{-13}$ around each x value, numerically convergent results were found using 100 bits in the significand. Figure 2 and Table 1 show that in this case, the linear approximation for the residual acceleration, $4\zeta(3)(M/L^3)x$, is accurate to within 10% over about three orders of magnitude. Near the halfway point and at $x > 0.5$, i.e. closer to the “next” image of the massive object than the “local” copy, the residual term defined in relation to the acceleration towards the “local” copy is clearly no longer small—it diverges as the test particle approaches the “next” copy. Thus, for $L \sim 10$ to $20h^{-1}$ Gpc, the linear expression should be accurate on scales of $3h^{-1}$ Mpc $\lesssim x \lesssim 2h^{-1}$ Gpc in a slab-space universe containing just one cluster of about $10^{14}M_{\odot}$.

4. Discussion

We have found that the topological acceleration effect is relativistically valid in (at least) the Schwarzschild-like slab space. Does this have implications regarding the accuracy of N -body simulations of the gravitational collapse of large-scale structure and the cosmic web? Farrar and Melott (1990) briefly showed that density fluctuation evolution on the largest scales of an N -body simulation is affected by cosmic topology, at least in the two-dimensional case. Here we are concerned with the accelerations on individual particles, which can be used as a first step towards understanding the effect found by Farrar and Melott (1990).

N -body simulations (e.g., Bagla, 2005; Dehnen and Read, 2011, and references therein) are generally made assuming a T^3 model for comoving space, typically with a universe size L that is smaller than is observationally realistic. The algorithms are typically developed with the aim of considering large-scale effects induced by the global topology to be artefacts, i.e. the aim is to ignore the physical effects of cosmic topology. The most frequently used approach is to use Fourier techniques either explicitly, with a particle mesh, or implicitly, using Ewald summation in a tree code (e.g. Hernquist et al., 1991). In Roukema et al. (2007) and Roukema and Rózański (2009) it was shown that for the Newtonian-like calculation of topological acceleration, the linear terms induced by topological images in different directions cancel each other exactly in a regular T^3 model, leaving topological acceleration that is dominated by a term that is cubical in x/L . In a T^3 model of unequal side lengths, a linear term in the shortest compact direction dominates.

Thus, to the degree to which they are numerically accurate, the most frequently used N -body methods eliminate the linear x/L topological acceleration term, leaving cubical $(x/L)^3$ terms. There has recently been considerable observational interest in T^3 candidate FLRW models (Spergel et al., 2003; Aurich et al., 2007; Aurich, 2008; Aurich et al., 2008, 2010; Aslanyan and Manohar, 2011), so for this case, standard N -body simulations could be analysed in detail in order to study the expected effects of topological acceleration on galaxy kinematics, in the nearly-Newtonian approximation. Since the effect is anisotropic, alignments with the fundamental directions (x, y, z axis directions of the simulation box) and vectorial calculations (Roukema et al., 2007) could be used to distinguish topological effects from numerical effects.

On the other hand, except for well-proportioned FLRW models (Weeks et al., 2004), the unequal lengths of comoving closed spatial geodesics in different directions imply that the linear term in x/L should dominate in a “typical” multiply connected FLRW model. Standard N -body simulation methods would need to be modified in order to study topological acceleration effects in these cases. Since the standard methods are based on either explicit or implicit Fourier techniques, relatively minor modifications of these might be enough to study both T^1 slab spaces and the T^2 model favoured by Aslanyan and Manohar (2011).

For FLRW models with even a small amount of curvature (e.g. a total den-

sity parameter of $\Omega_{\text{tot}} = 1.015$), especially the Poincaré dodecahedral space S^3/I^* (Luminet et al., 2003; Aurich et al., 2005*a,b*; Gundermann, 2005; Caillerie et al., 2007; Roukema, Buliński, Szaniewska and Gaudin, 2008; Roukema, Buliński and Gaudin, 2008), standard N -body simulations are incorrect for several reasons. Firstly, $\Omega_{\text{tot}} \neq 1$ does not only affect scale factor evolution $a(t)$, it also corresponds to curved comoving space. Secondly, the fundamental domain is, in general, not cubical, and even in cases where a cubical fundamental domain can be used (Aurich et al., 2011), the identification of faces is different from that in the T^3 model normally assumed for N -body simulations. Thus, Fourier techniques cannot be applied, although they could be replaced by harmonic analysis that uses orthonormal sets of basis functions that are less trivial than the sinusoidal basis functions used in Fourier techniques.

In contrast to models in which the acceleration is linear, i.e. stronger than in T^3 , both the linear and cubical terms cancel in the Poincaré space (Roukema and Rózański, 2009), leaving a dominant fifth order term. In this case, correctly designed N -body simulations should show topological acceleration effects that are *weaker* than in the standard simulations.

Thus, in order for N -body simulations to be used to develop methods of constraining the topology of the Universe independent of multiple imaging methods, the simulation design and algorithms would need to be modified in ways that should lead to topological acceleration that in “typical” FLRW models should be stronger than for the T^3 case, and in the Poincaré dodecahedral space weaker than for T^3 .

5. Conclusion

The T^1 (slab space) heuristic result is found to exist in the limit of the Schwarzschild-like, exact, slab-space solution of the Einstein equations found by Korotkin and Nicolai (1994), with the same linear topological acceleration term as for the simpler calculation. For a fundamental domain size of L , a slow-moving [Eq. (3)], low-mass test particle lying at distance $x \ll L/2$ along the axis [$\rho = 0$, Eq. (4)] from the object of positive mass $GM/c^2 \ll x$ [Eq. (2)] to its nearest multiple image, the additional acceleration away from the massive object is $4\zeta(3)G(M/L^3)x$ [Eq. (25)]. For a topological acceleration term away from a cluster of $\sim 10^{14}M_\odot$ and a Universe of size \ddagger $L \sim 10$ to $20h^{-1}$ Gpc, the linear expression should be accurate over $3h^{-1}$ Mpc $\lesssim x \lesssim 2h^{-1}$ Gpc (Fig. 2, column with $M = 3 \times 10^{-10}$ in Table 1). Thus, at least in a simple example of a multiply connected universe, the topological acceleration effect is not an artefact of Newtonian-like reasoning. The linear term exists as an analytical limit of the relativistic model and as a good numerical approximation to it over several orders of magnitude of x .

This qualitatively suggests that the Newtonian-like derivations of the topological acceleration effect for well-proportioned FLRW models (Roukema and Rózański, 2009), in which the Poincaré dodecahedral space is found to be uniquely well-balanced, might

\ddagger More formally, twice the injectivity radius, or twice the in-radius (Fig. 10, Luminet and Roukema, 1999, and references therein).

also be valid limits of fully relativistic Schwarzschild-like solutions with these spatial sections. Other extensions of the present work within the slab-space solution could include consideration of test particles with high coordinate velocities [violating Eq. (3)], or expanding (FLRW-like) solutions.

Acknowledgments

Use was made of the Centre de Données astronomiques de Strasbourg (<http://cdsads.u-strasbg.fr>), the GNU multi-precision (GMP) and MPFR libraries, and the GNU OCTAVE command-line, high-level numerical computation software (<http://www.gnu.org/software/octave>).

References

- de Sitter W 1917 *MNRAS* **78**, 3–28.
- Friedmann A 1923 *Mir kak prostranstvo i vremya (The Universe as Space and Time)* Leningrad: Academia.
- Friedmann A 1924 *Zeitschr. für Phys.* **21**, 326.
- Lemaître G 1927 *Annales de la Société Scientifique de Bruxelles* **47**, 49–59.
- Robertson H P 1935 *ApJ* **82**, 284.
- Lemaître G 1931 *MNRAS* **91**, 483–490.
- Seriu M 1996 *Phys. Rev. D* **53**, 6902, [arXiv:gr-qc/9603002v1].
- Anderson M, Carlip S, Ratcliffe J G, Surya S and Tschantz S T 2004 *CQG* **21**, 729, [arXiv:gr-qc/0310002].
- Dowker F and Surya S 1998 *Phys. Rev. D* **58**, 124019, [arXiv:gr-qc/9711070].
- Roukema B F and Kazimierczak T A 2011 *A&A* **533**, A11, [arXiv:1106.0727].
- Roukema B F, Bajtlik S, Biesiada M, Szaniewska A and Jurkiewicz H 2007 *A&A* **463**, 861–871, [arXiv:astro-ph/0602159].
- Roukema B F and Rózański P T 2009 *A&A* **502**, 27, [arXiv:0902.3402].
- Roukema B F 2002 *in* V G Gurzadyan, R T Jantzen, & R Ruffini, ed., ‘The Ninth Marcel Grossmann Meeting’ Singapore: World Scientific pp. 1937–1938, [arXiv:astro-ph/0010189].
- Célérier M, Bolejko K and Krasiński A 2010 *A&A* **518**, A21+, [arXiv:0906.0905].
- Buchert T and Carfora M 2003 *Phys. Rev. Lett.* **90**(3), 031101, [arXiv:gr-qc/0210045].
- Wiegand A and Buchert T 2010 *Phys. Rev. D* **82**(2), 023523, [arXiv:1002.3912].
- Korotkin D and Nicolai H 1994 *ArXiv General Relativity and Quantum Cosmology e-prints*, [arXiv:gr-qc/9403029].

- Frolov A V and Frolov V P 2003 *Phys. Rev. D* **67**(12), 124025, [arXiv:hep-th/0302085].
- Farrar K A and Melott A L 1990 *Computers in Physics* **4**, 185–189.
- Bagla J S 2005 *Current Science* **88**, 1088–1100, [arXiv:astro-ph/0411043].
- Dehnen W and Read J I 2011 *European Physical Journal Plus* **126**, 55, [arXiv:1105.1082].
- Hernquist L, Bouchet F R and Suto Y 1991 *ApJSupp* **75**, 231–240.
- Spergel D N, et al. 2003 *ApJSupp* **148**, 175, [arXiv:astro-ph/0302209].
- Aurich R, Lustig S, Steiner F and Then H 2007 *CQG* **24**, 1879–1894, [arXiv:astro-ph/0612308].
- Aurich R 2008 *CQG* **25**, 225017, [arXiv:0803.2130].
- Aurich R, Janzer H S, Lustig S and Steiner F 2008 *Classical and Quantum Gravity* **25**(12), 125006, [arXiv:0708.1420].
- Aurich R, Lustig S and Steiner F 2010 *CQG* **27**, 095009, [arXiv:0903.3133].
- Aslanyan G and Manohar A V 2011 *ArXiv e-prints* , [arXiv:1104.0015].
- Weeks J, Luminet J P, Riazuelo A and Lehoucq R 2004 *MNRAS* **352**, 258, [arXiv:astro-ph/0312312].
- Luminet J, Weeks J R, Riazuelo A, Lehoucq R and Uzan J 2003 *Nature* **425**, 593, [arXiv:astro-ph/0310253].
- Aurich R, Lustig S and Steiner F 2005a *CQG* **22**, 3443, [arXiv:astro-ph/0504656].
- Aurich R, Lustig S and Steiner F 2005b *CQG* **22**, 2061, [arXiv:astro-ph/0412569].
- Gundermann J 2005 *ArXiv e-prints* , [arXiv:astro-ph/0503014].
- Caillerie S, Lachièze-Rey M, Luminet J P, Lehoucq R, Riazuelo A and Weeks J 2007 *A&A* **476**, 691, [arXiv:0705.0217v2].
- Roukema B F, Buliński Z, Szaniewska A and Gaudin N E 2008 *A&A* **486**, 55, [arXiv:0801.0006].
- Roukema B F, Buliński Z and Gaudin N E 2008 *A&A* **492**, 673, [arXiv:0807.4260].
- Aurich R, Kramer P and Lustig S 2011 *ArXiv e-prints* , [arXiv:1107.5214].
- Luminet J and Roukema B F 1999 in M Lachièze-Rey, ed., ‘NATO ASIC Proc. 541: Theoretical and Observational Cosmology. Publisher: Dordrecht: Kluwer,’ p. 117, [arXiv:astro-ph/9901364].